# Low-energy magnetic dipole strength in cadmium isotopes

Schwengner, R.;

Originally published:

January 2022

**Physical Review C 105(2022), 014303**

DOI: https://doi.org/10.1103/PhysRevC.105.014303

# Low-energy magnetic dipole strength in cadmium isotopes

R. Schwengner
*Helmholtz-Zentrum Dresden-Rossendorf, 01328 Dresden, Germany*
(Dated: October 15, 2021)

Magnetic dipole strength functions have been deduced from averages of large numbers of $M1$ transition strengths calculated within the shell model for the nuclides $^{105}$Cd, $^{106}$Cd $^{111}$Cd, and $^{112}$Cd. Enhancements of the $M1$ strengths toward low transition energy have been found for all nuclides considered. These properties are compared with those of experimental photon strength functions obtained from $^{3}$He-induced reactions, which seem to indicate a disappearance of the low-energy enhancement in the heavier isotopes.

PACS numbers: 21.10.Pc, 21.60.Cs, 23.20.Lv, 27.50.+e

## I. INTRODUCTION

The investigation of properties of $\gamma$-ray strength functions has been the subject of numerous experimental and theoretical works in the past years. By describing average transition strengths in a certain range of high excitation energy and high level density, $\gamma$-ray strength functions are a main input to calculations of reaction rates within statistical reaction models. These calculations are used, for example, to obtain information about neutron-capture cross sections of unstable nuclides. A number of new phenomena has been found on top of the low-energy tail of the isovector giant dipole resonance (GDR), such as the pygmy dipole resonance (PDR) between about 6 and 10 MeV consisting of electric dipole ($E1$) excitations [1–3], the scissors mode in deformed nuclides around 3 MeV based on magnetic dipole ($M1$) excitations [4], and the low-energy enhancement or so-called upbend, an increase of dipole strength with decreasing $\gamma$-ray energy below about 2 MeV. It was shown that the PDR affects neutron-capture rates determining the path of the astrophysical s-process of the nucleosynthesis [5, 6], while the pronounced enhancement of the dipole strength at low $\gamma$-ray energy may have a potentially large impact on neutron-capture reaction rates of very neutron-rich nuclides occurring in the r-process [7].

The low-energy enhancement has been observed in a number of nuclides in various mass regions, mainly using light-ion induced reactions in connection with the so-called Oslo method to extract level densities and $\gamma$-ray strength functions. These studies started with $^{56,57}$Fe [8] and continued to heavier nuclides, for example Ge isotopes [9], Y isotopes [10], Mo isotopes [11], Cd isotopes [12], and Sm isotopes [13, 14]. The Oslo method was also applied in connection with $\beta$ decay of $^{76}$Ga [15]. A dominant dipole character of the low-energy strength was demonstrated in Ref. [16] and an indication for an $M1$ character was discussed for the case of $^{60}$Ni [17]. An exceptional case is represented by the Cd isotopes. The light isotope $^{105}$Cd shows the upbend below about 1.5 MeV, whereas the strength functions of the neighbor $^{106}$Cd and of the heavier isotopes $^{111}$Cd and $^{112}$Cd do not show an upbend [12]. Possible reasons for this behavior, speculated in Ref. [12], may be the uncovering of a mass region exhibiting the onset of the low-energy enhancement.

To understand the mechanism producing the enhanced strength at low-energy, various model calculations have been performed. Shell-model calculations revealed that a large number of $M1$ transitions between excited states produces an exponential increase of the $\gamma$-ray strength function that peaks at $E_\gamma \approx 0$ and describes the low-energy enhancement of dipole strength observed in Mo isotopes around the neutron shell closure at $N = 50$ [18]. Large $B(M1)$ transition strengths appear for transitions linking states with configurations dominated by both protons and neutrons in high-$j$ orbits, the spins of which recouple. The low-energy enhancement of $M1$ strength was confirmed in shell-model calculations for $^{56,57}$Fe [19] and $^{44,46}$Ti [20]. In the latter work, also the $E1$ strength function was calculated, which does not show an upbend comparable to that of the $M1$ strength. A correlation between the low-energy $M1$ strength and the scissors mode was found in shell-model calculations for the series of isotopes from $^{60}$Fe to $^{68}$Fe [21]. The low-energy $M1$ strength decreases and the scissors strength develops when going into the open shell. The simultaneous appearance of the two modes is in accordance with experimental findings in Sm isotopes [13, 14]. Later on, $M1$ strength functions have been calculated for isotopic series in several mass regions from $Z = 8$ to 32 [22, 23] and $Z = 52$ to 58 [24]. These shell-model studies confirmed that the low-energy enhancement of $M1$ strength appears in almost all nuclides studied and is strongest in nuclides near shell closures. The only cases without a low-energy enhancement are the $N = Z$ nuclides $^{48}$Cr [25] and $^{108}$Xe [24].

With respect to those results, the trends of the strength functions observed in the Cd isotopes remain an open issue for the understanding of the occurrence of the low-energy enhancement as a general feature. As an approach to this problem, the present work presents predictions of shell-model calulations for the $M1$ strength functions of the Cd isotopes and confronts these with the experimental findings.

## II. SHELL-MODEL CALCULATIONS

The shell-model calculations for the cadmium isotopes were carried out in the jj45pn model space with the jj45pna Hamiltonian [26, 27] using the code NuShellX@MSU [28]. The Hamiltonian was not specifically adjusted to the isotopes considered here. The model space included the proton orbits $(1f_{5/2}, 2p_{3/2}, 2p_{1/2}, 1g_{9/2})$ and the neutron orbits $(1g_{7/2}, 2d_{5/2}, 2d_{3/2}, 2s_{1/2}, 1h_{11/2})$. To make the calculations feasible, the configuration spaces were truncated. Two protons were allowed to be excited from the $(fp)$ orbitals to the $1g_{9/2}$ orbital. In $^{105}$Cd and $^{106}$Cd, at least three neutrons occupied the $1g_{7/2}$ and at least two the $2d_{5/2}$ orbital. One neutron could be lifted to each of the $(2d_{3/2}, 2s_{1/2})$ orbitals and up to two to the $1h_{11/2}$ orbital. In $^{111}$Cd and $^{112}$Cd, at least six neutrons occupied the $1g_{7/2}$ and at least four the $2d_{5/2}$ orbital. Up to two neutrons could be lifted to each of the $(2d_{3/2}, 2s_{1/2}, 1h_{11/2})$ orbitals. Reduced electric quadrupole transition strengths $B(E2)$ were calculated applying effective charges of $e_\pi = 1.6e$ and $e_\nu = 1.0e$ as used in recent calculations of $B(E2)$ values between low-lying states in $^{106}$Cd [29].

The $2_1^+$ state in $^{106}$Cd was calculated at $E(2_1^+)_{\rm calc} = 0.480$ MeV, compared to an experimental value of $E(2_1^+)_{\rm exp} = 0.633$ MeV. The calculated strength of the ground-state transition, $B(E2, 2_1^+ \rightarrow 0_1^+)_{\rm calc} = 718$ $e^2$fm$^4$, is compatible with the experimental value of $B(E2, 2_1^+ \rightarrow 0_1^+)_{\rm exp} = 769(9)$ $e^2$fm$^4$. The corresponding values for $^{112}$Cd are $E(2_1^+)_{\rm calc} = 0.468$ MeV, $E(2_1^+)_{\rm exp} = 0.618$ MeV, $B(E2, 2_1^+ \rightarrow 0_1^+)_{\rm calc} = 905$ $e^2$fm$^4$, and $B(E2, 2_1^+ \rightarrow 0_1^+)_{\rm exp} = 972(6)$ $e^2$fm$^4$. In the heavier isotopes, more than two neutrons may be lifted to the $1h_{11/2}$ orbital. To enable this in the calculations, stronger limitations have to be applied to the other neutron orbitals. With at least five neutrons in the $2d_{5/2}$ orbital, at most one in each of the $(2d_{3/2}, 2s_{1/2})$ orbitals and still up to two in the $1h_{11/2}$ orbital, one obtains a reduction of the $B(E2, 2_1^+ \rightarrow 0_1^+)_{\rm calc}$ value to 692 $e^2$fm$^4$ in $^{112}$Cd. At the same time, the low-energy $M1$ upbend gets steeper and the peak near $E_\gamma = 0$ increases by a factor of about two. Such an increase is a typical effect appearing when making the configuration space small. Allowing up to three neutrons in the $1h_{11/2}$ orbital along with the other limitations just mentioned, one obtains similar values, $B(E2, 2_1^+ \rightarrow 0_1^+)_{\rm calc} = 634$ $e^2$fm$^4$ and a slightly higher peak of the upbend near $E_\gamma = 0$, while the mean neutron numbers in the $1h_{11/2}$ orbital do not considerably exceed the number of two in most states. The calculations described in the following refer to the limitations given first in this section.

The calculations were performed for the lowest 40 states of each spin from 0 to 10 and each parity. Reduced magnetic dipole transition strengths $B(M1)$ were calculated applying effective $g$ factors of $g_s^{\rm eff} = 0.7 g_s^{\rm free}$ for all transitions from initial to final states with energies $E_i > E_f$ and spins $J_i = J_f, J_f \pm 1$. This resulted in about 24000 $M1$ transitions. $M1$ strength functions were deduced according to

$$f_{M1}(E_\gamma, E_i, J_i, \pi) = \\ 16\pi/9\ (\hbar c)^{-3}\ \overline{B}(M1, E_i \rightarrow E_f, J_i, \pi)\ \rho(E_i, J_i, \pi), \quad (1)$$

with $E_\gamma = E_i - E_f$, where the $\overline{B}(M1, E_i \rightarrow E_f, J_i, \pi)$ are averages in considered $(E_i, E_f)$ bins for given $J_i$, $\pi$, and $\rho(E_i, J_i, \pi)$ are level densities derived from the present calculations. The strength functions $f_{M1}(E_\gamma)$ were obtained by averaging step-by-step over $E_i$, $J_i$, and $\pi$.

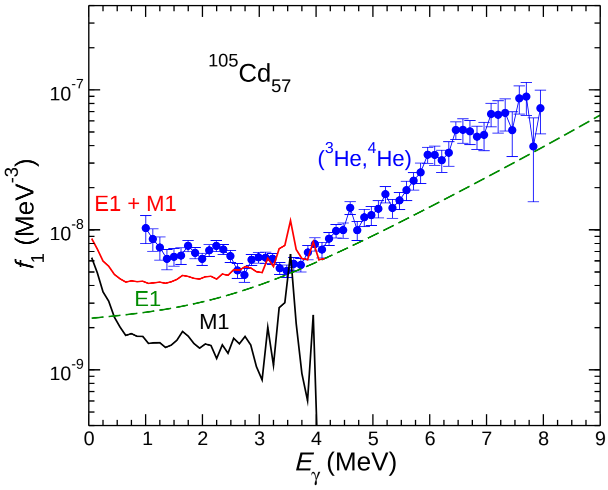


FIG. 1: $M1$ strength function for $^{105}$Cd deduced from the present shell-model calculations (black solid line), $E1$ strength function based on the GLO model (green dashed line), the sum of the $M1$ and $E1$ strength functions (red solid line), and experimental data from $^3$He-induced reactions (blue circles).

## III. RESULTS

For a comparison with the experimental dipole strength functions $f_1$ determined in Ref. [12], an $E1$ part had to be added to the present calculated $M1$ strength functions. As the data in Ref. [12] were compared with the generalized Lorentzian (GLO) model [30, 31], this was also used here with identical parameters for the $E1$ strength. The $M1$ and $E1$ strength functions as well as their sums are graphed for the considered isotopes in Figs. 1, 2, 3, and 4.

The $M1$ strength functions in all four isotopes show an enhancement toward $E_\gamma = 0$ below about 1 MeV. Toward high energy, the upbend is followed by a saddle and a bump between about 2 and 4 MeV. This bump corresponds to the one seen in open-shell Fe [21] and Sm isotopes [13, 14] and is considered as a scissorslike resonance. Prominent peaks in the high-energy part of the $M1$ strength function arise from strong transitions from the highest calculated levels to the ground or first excited states. These dominate the average strength because of

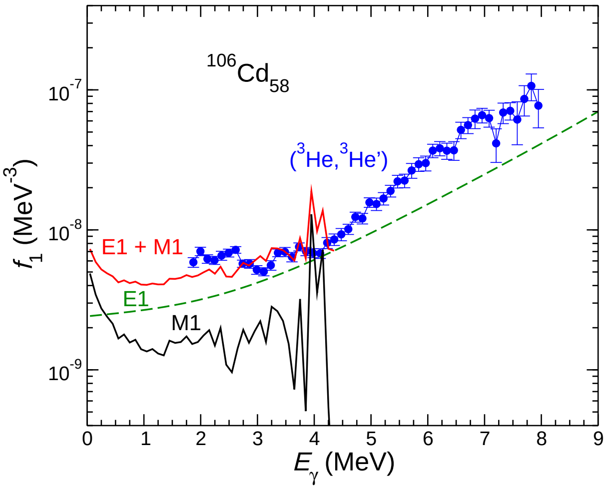


FIG. 2: As Fig. 1, but for $^{106}$Cd.

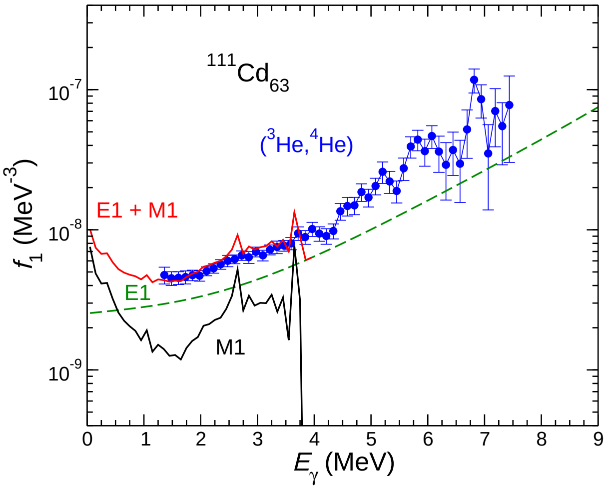


FIG. 3: As Fig. 1, but for $^{111}$Cd.

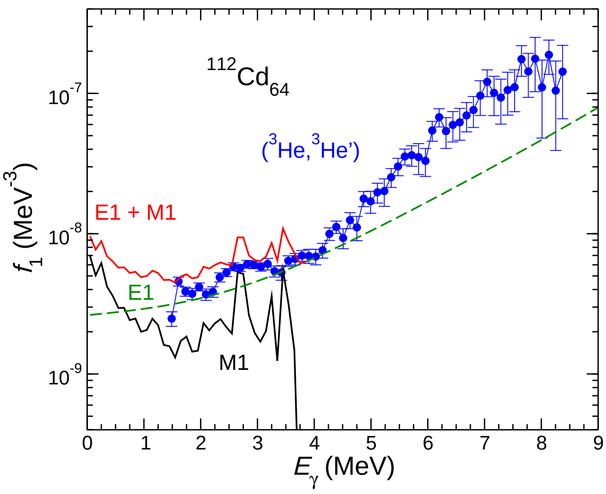


FIG. 4: As Fig. 1, but for $^{112}$Cd.

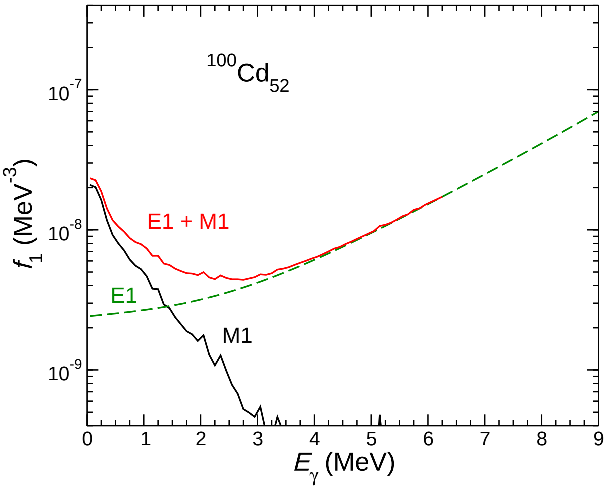


FIG. 5: As Fig. 1, but for $^{100}$Cd. There are no experimental data available for this nuclide.

the small number of transitions in the highest energy bins and hence overestimate the $M1$ strength function at the upper end of the calculated spectrum. All total $(E1 + M1)$ strength functions $f_1$ also exhibit the low-energy enhancement. In $^{105}$Cd, the calculated $f_1$ lies below the experimental one. Besides, the enhancement starts below about 0.7 MeV, whereas the experimental one reaches to about 1.5 MeV. In $^{106}$Cd, calculated and experimental $f_1$ behave similarly between about 2 and 4 MeV. There are no experimental data below about 2 MeV and hence no information about a possible upbend. In the heavier isotope $^{111}$Cd, a good agreement of calculated and experimental $f_1$ is seen between about 1.5 and 4 MeV. Also in this isotope the upbend in the calculated $f_1$ starts where the experimental data stop. In $^{112}$Cd, a beginning upbend may be indicated by the three experimental values below 2 MeV, but the value at the lowest energy is considerably smaller in contrast to the calculated $f_1$ that starts to increase at about this energy.

To reveal the development of the low-energy $M1$ strength with nucleon numbers approaching shell closures, the $M1$ strength function was also calculated for the $N = 52$ isotope $^{100}$Cd. The results are shown in Fig. 5. The $f_{M1}$ reaches about twice the magnitude at $E_\gamma \approx 0$ compared with the heavier isotopes. It shows a steady decrease toward high energies, while the bump between 2 and 4 MeV seen in the heavier isotopes disappears. The increase of the low-energy strength and the disappearance of the scissorslike resonance when approaching shell closures is consistent with the properties found for the series of Fe isotopes [21].

## IV. CONCLUSIONS

$M1$ strength functions deduced from shell-model calculations for the isotopes $^{100}$Cd, $^{105}$Cd, $^{106}$Cd, $^{111}$Cd, and $^{112}$Cd do not confirm a disappearance of the low-energy enhancement of dipole strength in the heavier isotopes, which was suspected on the basis of experimental data. The low-energy enhancement of $M1$ strength is present in all isotopes. However, it gets weaker when going into the open neutron shell, while a bump develops in the region of the scissors resonance. This behavior resembles the properties of $M1$ strength found in other mass regions. Except for $^{105}$Cd, the calculated low-energy upbend is below the lowest energies, for which experimental data are available. Therefore, a definite conclusion about the appearance of the upbend is not possible on the basis of the existing data. A more comprehensive study of the behavior of the strength functions at very low energy in $^{111}$Cd and $^{112}$Cd on the basis of new high-resolution experiments may clarify the situation.

## V. ACKNOWLEDGMENTS

I thank K. Sieja for stimulating discussions and B. A. Brown for his support in using the code NuShellX@MSU. The allocation of computing time through the Centers for High-Performance Computing of Technische Universität Dresden and of Helmholtz-Zentrum Dresden-Rossendorf is gratefully acknowledged.

[1] G. A. Bartholomew, E. D. Earle, A. J. Ferguson, J. W. Knowles, and M. A. Lone, in *Advances in Nuclear Physics*, edited by M. Baranger and E. Vogt, Vol. 7 (Springer, Boston, MA, 1973), pp. 229 - 324.
[2] D. Savran, T. Aumann, and A. Zilges, Prog. Part. Nucl. Phys. **70**, 210 (2013).
[3] A. Bracco, E. G. Lanza, and A. Tamii, Prog. Part. Nucl. Phys. **106**, 360 (2019).
[4] K. Heyde, P. von Neumann-Cosel, and A. Richter, Rev. Mod. Phys. **82**, 2365 (2010).
[5] M. Beard, S. Frauendorf, B. Kämpfer, R. Schwengner, and M. Wiescher, Phys. Rev. C **85**, 065808 (2012).
[6] N. Tsoneva, S. Goriely, H. Lenske, and R. Schwengner, Phys. Rev. C **91**, 044318 (2015).
[7] A. C. Larsen and S. Goriely, Phys. Rev. C **82**, 014318 (2010).
[8] A. Voinov *et al.*, Phys. Rev. Lett. **93**, 142504 (2004).
[9] T. Renstrøm *et al.*, Phys. Rev. C **93**, 064302 (2016).
[10] A. C. Larsen *et al.*, Phys. Rev. C **93**, 045810 (2016).
[11] M. Guttormsen *et al.*, Phys. Rev. C **71**, 044307 (2005).
[12] A. C. Larsen *et al.*, Phys. Rev. C **87**, 014319 (2013).
[13] A. Simon *et al.*, Phys. Rev. C **93**, 034303 (2016).
[14] F. Naqui *et al.*, Phys. Rev. C **99**, 054331 (2019).
[15] A. Spyrou *et al.*, Phys. Rev. Lett. **113**, 232502 (2014).
[16] A. C. Larsen *et al.*, Phys. Rev. Lett. **111**, 242504 (2013).
[17] A. Voinov *et al.*, Phys. Rev. C **81**, 024319 (2010).
[18] R. Schwengner, S. Frauendorf, and A. C. Larsen, Phys. Rev. Lett. **111**, 232504 (2013).
[19] B. Alex Brown and A. C. Larsen, Phys. Rev. Lett. **113**, 252502 (2014).
[20] K. Sieja, Phys. Rev. Lett. **119**, 052502 (2017).
[21] R. Schwengner, S. Frauendorf, and B. A. Brown, Phys. Rev. Lett. **118**, 092502 (2017).
[22] S. Karampagia, B. A. Brown, and V. Zelevinsky, Phys. Rev. C **95**, 024322 (2017).
[23] J. E. Midtbø, A. C. Larsen, T. Renstrøm, F. L. Bello Garrote, and E. Lima, Phys. Rev. C **98**, 064321 (2018).
[24] K. Sieja, Phys. Rev. C **98**, 064312 (2018).
[25] K. Sieja, EPJ Web. Conf. **146**, 05004 (2017).
[26] M. Honma, T. Otsuka, B. A. Brown, and T. Mizusaki, Phys. Rev. C **69**, 034335 (2004).
[27] M. Honma, T. Otsuka, B. A. Brown, and T. Mizusaki, Eur. Phys. J. A **25**, Suppl. 1, 499 (2005).
[28] B. A. Brown and W. D. M. Rae, Nucl. Data Sheets **120**, 115 (2014).
[29] D. Rhodes *et al.*, Phys. Rev. C **103**, L051301 (2021).
[30] J. Kopecky and R. E. Chrien, Nucl. Phys. A **468**, 285 (1987).
[31] J. Kopecky and M. Uhl, Phys. Rev. C **41**, 1941 (1990).